NUMERICAL AND EXPERIMENTAL INVESTIGATION OF COLD ROTARY SWAGED TI ALLOY

BAGHIROVA Banovsha[1], ŠOFER Michal [2], STRUNG Václav [3]

[1]VSB - Technical University of Ostrava, Department of Materials Forming, Czech Republic, EU, banovsha.baghirova.st@vsb.cz
[2]VSB - Technical University of Ostrava, Department of Applied Mechanics, Czech Republic, EU, michal.sofer@vsb.cz
[3]VSB - Technical University of Ostrava, Regional Materials Science and Technology Centre, Czech Republic, EU, vaclav.strung.st@vsb.cz

Abstract

The aim of our study was to investigate the cold rotary swaging on the Ti6Al4V alloy with a finite element modelling (FEM) and subsequently by experimental verification of the model predictions. The experimental examination was evaluated both cast and swaged material states. A FEM analysis was performed to describe the rotary swaging from a 7.5 mm round bar diameter with the total reduction of 27 % in cross-section. The numerical simulations were focused on the investigation of swaging force, distributions of strain, stress state, temperature and plastic flow of material. Subsequent experimental verification such as microhardness, tensile properties, and microstructure observations validated the predicted results. The one of experimental analysis was dedicated on measurement of swaging force during RS by using KOMAFU S600 dynamical force measuring system. After comparison between predicted and experimentally obtained data a good agreement was found. Among others there was observed same trend between microhardness profile and imposed strain distribution throughout the cross section of swaged billet.

Keywords: Cold rotary swaging, Ti6Al4V, mechanical properties, numerical modelling

1. INTRODUCTION

Rotary swaging (RS) is a forming technology characterized by a high surface quality of the final products, materials savings and short productions times. The process is very often used to produce rods, tubes, and wires, as well as asymmetrical products, under cold, as well as hot conditions. As regards the processed materials, RS can be applied to impart plastic deformation to virtually any deformable material, which can be either cast [1], or produced via powder metallurgy technologies [2]. Advantageously, RS can be used to process materials with a relatively low formability, such as Mg alloys [3].

This forming technology has primarily been designed to reduce cross-sections of solid and hollow work-pieces. It has already been investigated from various viewpoints, such as distribution of strain and stress within the formed material, influence of axial velocity of the infeed work-piece on strain distribution, influence of friction on deformation behaviour, influence of the inlet angle of swaging dies on distribution of residual stresses and temperature etc. [4-9]. However, characterization of plastic flow during RS is quite a complex issue, since the strain intensity and vector change after each individual stroke [7]. Despite the fact that the material should primarily flow in the axial direction, this presupposition cannot be generalized. Similarly complex is determination of swaging forces.

Titanium and its alloys are nowadays widely used for many different applications, such as medical prostheses, orthopaedic implants, dental and endodontic instruments and files, dental implants, aerospace and military components, automotive components, agri-food, sporting goods, jewellery, components of mobile phones, etc. [10-13].

This paper deals with a numerical modelling and subsequent experimental verification of cold rotary swaging of Ti6Al4V. The main focus was on characterization of deformation behaviour - distributions of effective strain and temperature, swaging force and mechanical properties of the swaged alloy.

2. EXPERIMENT DESCRIPTION

The first part of the study, the numerical analysis, was realized by applying FORGE NxT commercial software, the assembly for which is depicted in **Figure 1a**. The boundary conditions of the numerical analysis corresponded to the experimental conditions (material, geometry of dies and work-piece, initial work-piece temperature, swaging speed etc.). The analysed Ti alloy had the composition of (in wt. %) 6 - Al, 3.91 - V, 0.125 - Fe, 0.115 - 0, 0.011 - C, 0.007 - N, bal. Ti. The initial work-piece diameter of 7.5 mm was reduced under room temperature (20 °C) by swaging down to the final diameter of 6.55 mm in a single pass with the reduction ratio of 0.27 (see **Figure 1b**). The friction between the work-piece and dies was defined using the Coulomb law with the friction coefficient of μ=0.1.

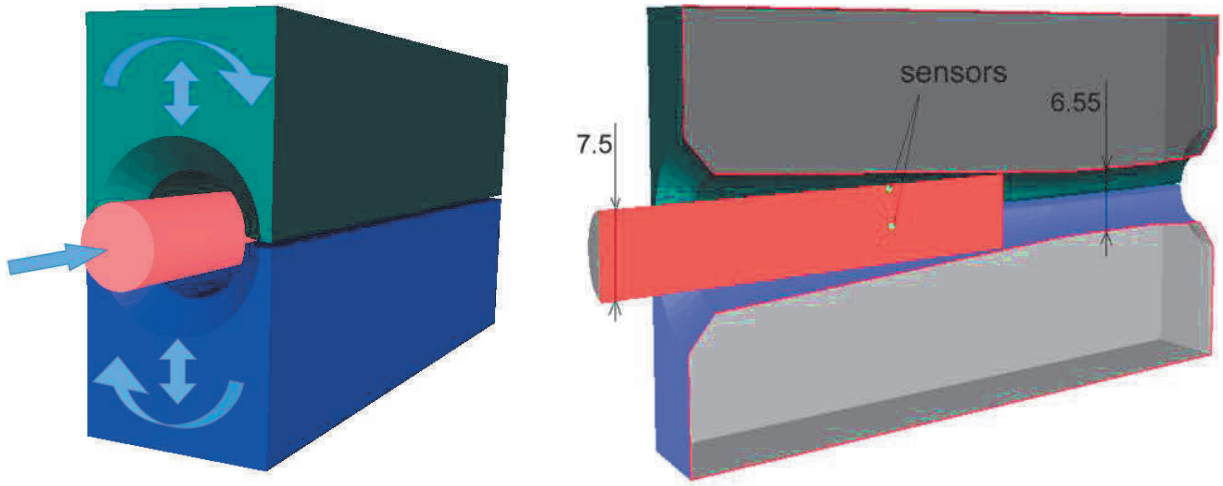

(a) geometry of the assembly (b) axial cut through the assembly

Figure 1 Scheme of assembly for rotary swaging

During the experimental swaging, swaging forces were recorded using the own designed KOMAFU S600 system for dynamic swaging force measurement [7]. The system comprises integrated measurement of temperature of the swaged-piece, which is favourable especially during hot swaging. Besides, mechanical properties were also examined via tensile tests performed with the use of a Testometric M500-50CT machine and Vickers microhardness measurements. Structures were evaluated via optical and scanning electron microscopy, for which the Quanta FEG 450 SEM equipment was used.

3. RESULT AND DISCUSSION

3.1. FEM Analyses

The results of the FEM analysis show a certain inhomogeneity of the imposed strain along the cross-section of the swaged-piece. The predicted values were the highest (~ 0.6) at the swaged-piece surface and decreased towards its axis (**Figure 2a**). This trend is given by the characteristics of the swaging process, during which the strain is imposed from the periphery towards the axis of the swaged-piece [4]. The final difference between the axial and surface regions from the viewpoint of strain values is depicted in **Figure 2b**, however, the effective strain gradient under these local surface layers was not significant.

On the other hand, the temperature distribution depicted in **Figure 2c** rather disagrees to the distribution of strain. Evidently, a significant increase in temperature occurred along the entire swaged-piece during swaging, the highest temperature in the swaged-piece axial region exceeded 140 °C. However, the temperature was lower in the peripheral part (**Figure 2d**). This behaviour was caused by the large contact area of the relatively

thin work-piece with the dies, which imparted a rapid heat transfer from the peripheral region of the swaged-piece.

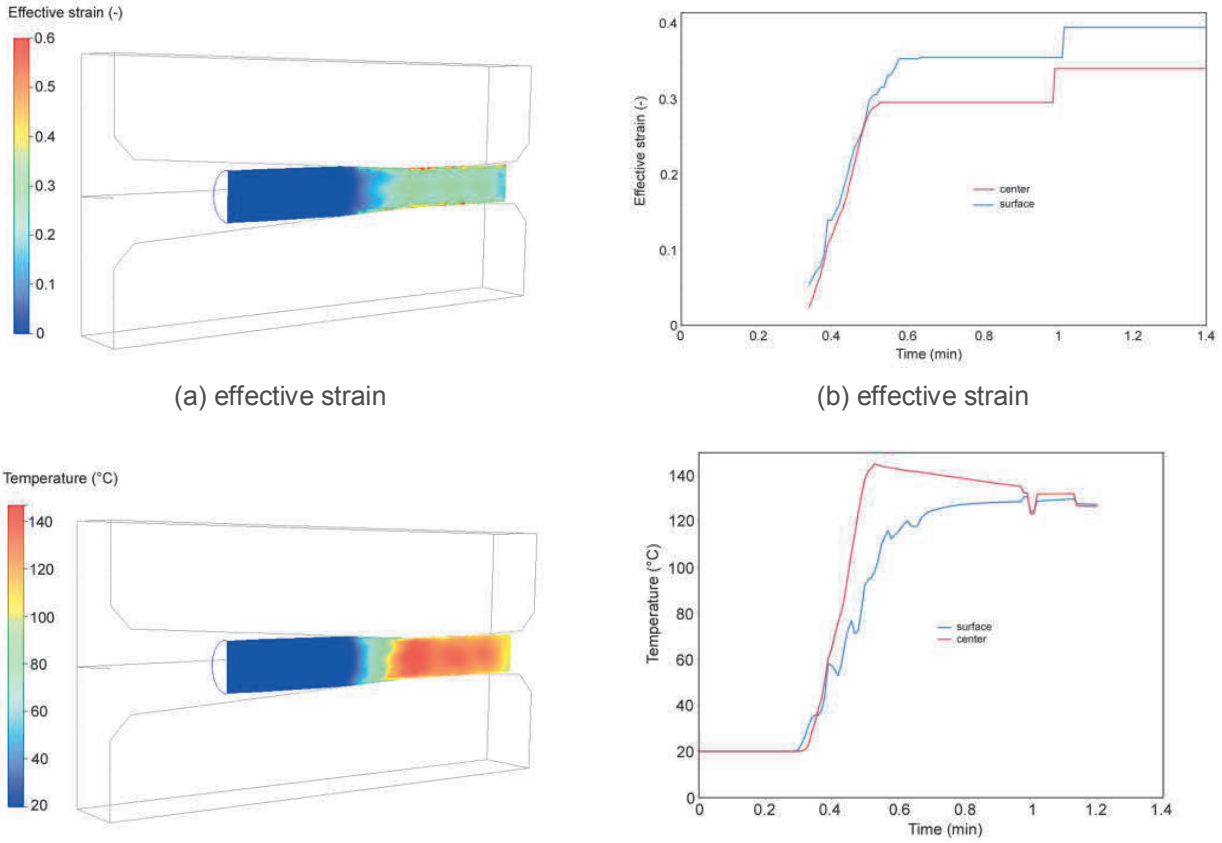

(a) effective strain

(b) effective strain

(c) temperature

(d) temperature

Figure 2 Deformation parameters in the central cutting plane of the swaged-piece

One of the most important parameters is the development of swaging force, the prediction of which is depicted in **Figure 3**. Evidently, a gradual force increase occurred in the early stages of swaging. The swaging force then reached its maximum value of approximately 200 kN when the dies were fully filled with the processed material. After reaching the maximum, the force gradually decreases again, which was directly connected with the reverse in plastic flow direction within the work-piece. This phenomenon can also be attributed to the influence of solid ends of the swaged-piece [7].

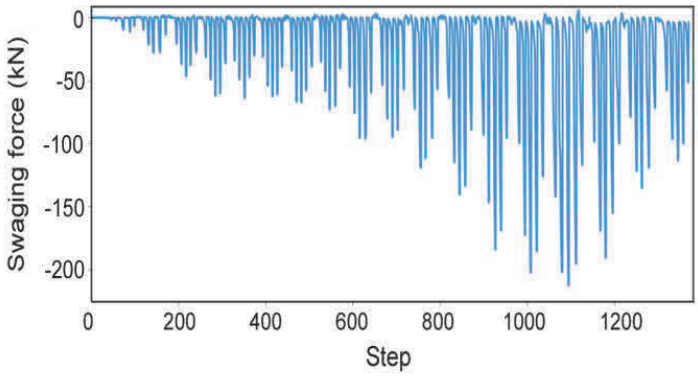

Figure 3 Predicted swaging force development

3.2. Experimental swaging

3.2.1. Microstructure

The microstructures of the Ti6Al4V alloy for both, the initial and swaged states, are depicted in **Figure 4**. The structure before swaging obviously consisted of non-uniform grains. However, the individual grain

boundaries could not be distinguished any more by OM after swaging. The imposed strain imparted quite a significant structure changes and grain refinement. By this reason, SEM was applied to investigate the swaged structure in a greater detail, as well as to analyse the chemical composition of the alloy.

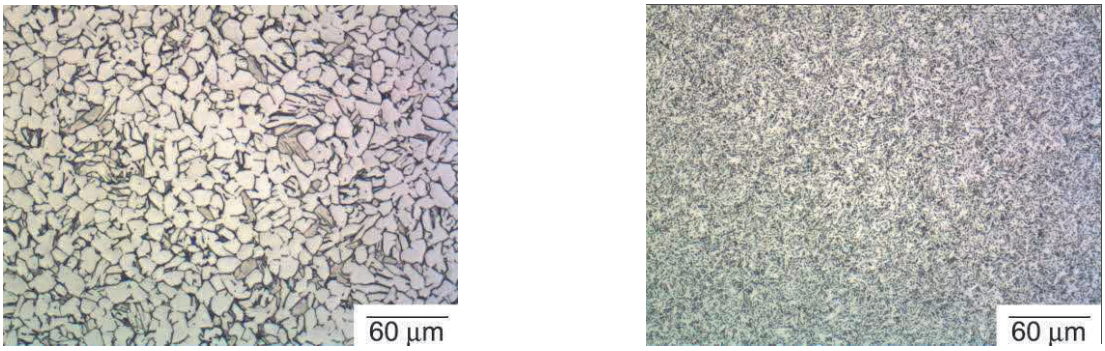

(a) before swaging (b) after swaging

Figure 4 Microstructures of Ti6Al4V

The chemical composition of the Ti6Al4V alloy was measured by EDS analyses, the locations for which can be seen in **Figure 5a**. While the grains within the alloy consisted mostly of Ti (**Figure 5b**), the inter-grain mass was defined by the chemical composition of 80.87 wt. % titanium, 3.13 wt. % aluminium and 16.00 wt. % vanadium.

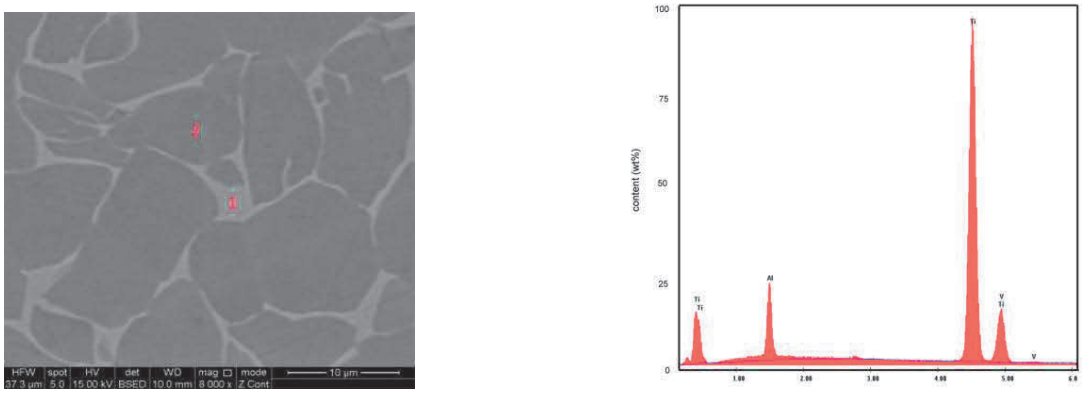

(a) localization of measured regions for EDS analysis (b) SEM analysis of grain

Figure 5 EDS and SEM analysis

3.2.2.Swaging force

The comparison of the swaging force recorded experimentally using the KOMAFU S600 system for dynamic force measurement and the predicted swaging force is depicted in **Figure 6**. The predicted and experimental results exhibited a satisfactory correlation, the experimental forces well corresponded to the predicted force development. The swaging force development thus confirmed validity of the used numerical model. The possible local deviations between both the results were caused primarily by the influences of several factors, such as the used mathematical model and meshing quality, the defined boundary condition for the simulation, possible structural inhomogeneity of the swaged-piece, variable friction during the swaging process, axial velocity of the swaged-piece, etc.

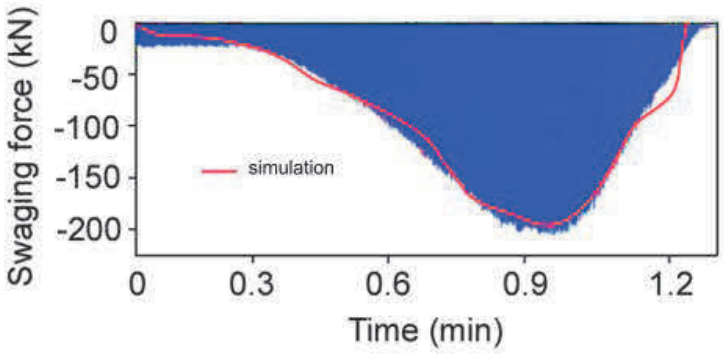

Figure 6 Comparison of experimental and predicted swaging forces

3.2.3. Mechanical properties

In order to characterize the influence of swaging on the formed Ti work-piece, mechanical properties were also examined. The first examination was via tensile testing; **Figure 7a** shows the stress-strain curves for the two material states before and after swaging, while the second type of examination was microhardness measurement, the results of which are shown in **Figure 7b**. As shown by **Figure 7a**, swaging imparted a significant increase in strength, however, plasticity decreased. This behaviour is typical for deformation strengthened materials [4, 14, 15]. On the other hand, the development of microhardness more or less corresponded to the predicted imposed strain (Section 3.1., **Figure 2b**).

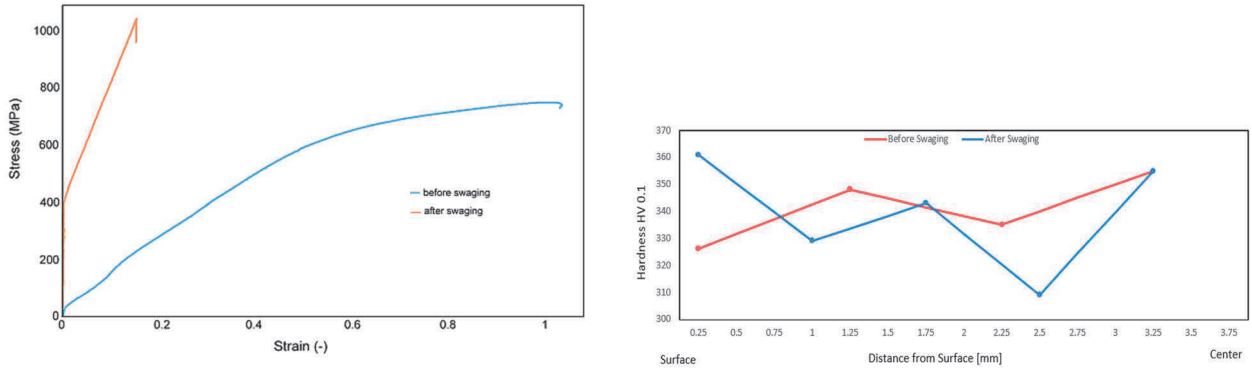

(a) stress-strain curves (b) microhardness development

Figure 7 Mechanical properties of investigated alloy for the two material states

4. CONCLUSIONS

This study was focused on the deformation behaviour of Ti6Al4V during cold rotary swaging. As was shown, this type of forming led to a significant increase in strength with relatively unsubstantial phase changes. One of the main goals was to determine the development of swaging force during the forming process. The performed numerical prediction enabled to determine the value and distribution of the imposed strain, as well as the temperature distribution within the swaged-piece. The comparison of the predicted and experimentally recorded swaging forces, both reaching to -200 kN, confirmed validity of the applied numerical model. The predicted results were in accordance with the experimental ones.

ACKNOWLEDGEMENTS

This paper was created within the research project no. SP2017/103 of VSB - Technical University of Ostrava, CZ and funded by INFINITY project in the framework of the EU Erasmus Mundus Action 2.

REFERENCES

[1] GAN, W.M., et al. Bulk and local textures of pure magnesium processed by rotary swaging. *Journal of Magnesium and Alloys,* 2013, vol. 1, no. 4, pp. 341-345.

[2] KUNCICKA, L., et al. Synthesis of an Al/Al2O3 composite by severe plastic deformation. *Journal of Materials Science Engineering,* 2015, vol. 646, no. 75, pp. 234-241.

[3] GAN, W.M., et al. Microstructures and mechanical properties of pure Mg processed by rotary swaging. *Journal of Material and Design,* 2014, vol. 63, no. 57, pp. 83-88.

[4] KOCICH, R., et al. Cold rotary swaging of a tungsten heavy alloy: Numerical and experimental investigations. *International Journal of Refractory Metals and Hard Materials,* 2016, vol. 61, no. 5, pp. 264-272.

[5] DOMBLESKY, J.P., SHIVPURI, R. Development and validation of a finite-element model for multiple-pass radial forging. *Journal of Materials Processing Technology,* 1995, vol. 55, no. 3-4, pp. 432-441.

[6] PIELA, A. Analysis of the metal flow in swaging - Numerical modelling and experimental verification. *International Journal of Mechanical Sciences,* 1997, vol. 39, no. 2, pp. 221-231.

[7] KOCICH, R., et al. Deformation behavior of multilayered Al-Cu clad composite during cold-swaging. *Journal of Materials & Design,* 2016, vol. 90, no.145, pp. 379-388.

[8] RONG, L., NIE, Z., ZUO, T. 3D finite element modeling of cogging-down rotary swaging of pure magnesium square billet - Revealing the effect of high-frequency pulse stroking. *Journal of Material Science and Engineering,* 2007, vol. 464, no. 1-2, pp. 28-37.

[9] AMELI, A., MOVAHHEDY, M. A parametric study on residual stresses and forging load in cold radial forging process. *International Journal of Advanced Manufacturing Technology,* 2007, vol. 33, no. 1, pp. 7-17.

[10] ZHAO, X. F., et al. Optimization of Cr content of metastable β-type Ti-Cr alloys with changeable Young's modulus for spinal fixation applications. *Acta Biomaterialia,* 2012, vol. 8, no. 6, pp. 2392-2400.

[11] KUNCICKA, L., KOCICH, R., LOWE, T.C. Advances in metals and alloys for joint replacement. *Journal of Progress in Materials Science,* 2017, vol. 88, no. 2, pp. 232-280.

[12] NIINOMI, M. Mechanical properties of biomedical titanium alloys. *Journal of Materials Science and Engineering,* 1998, vol. 243, no. 1-2, pp. 231-236.

[13] OCHONOGOR, O.F., AKINLABI, E.T., NYEMBWE, D. A review on the effect of creep and microstructural change under elevated temperature of Ti6Al4V alloy for Turbine engine Application. *Journal of Materials Today: Proceedings,* 2017, vol. 4, no. 2, pp. 250-256.

[14] KOCICH, R., et al. Fabrication and characterization of cold-swaged multilayered Al-Cu clad composites. *Journal of Materials & Design,* 2015, vol. 71, no. 8, pp. 36-47.

[15] DURLU, N., KAAN, C.N., SAKIR, B. Effect of swaging on microstructure and tensile properties of W-Ni-Fe alloys. *International Journal of Refractory Metals and Hard Materials,* 2014, vol. 42, no. 13, pp. 126-131.